

Calibration of Star Formation Rate Tracers with Population Synthesis Models: the L_X to L_{FIR} Ratio

Héctor Otí-Floranes¹ and Jose Miguel Mas-Hesse²

¹*LAEFF-INTA, POB 78, 28691 Villanueva de la Cañada, Spain*

²*Centro de Astrobiología (CSIC-INTA), 28850 Torrejón de Ardoz, Spain*

Abstract. The study of massive star formation needs some basic tools, among which reliable SFR tracers are crucial ones. We are presently revising the calibration of SFR tracers at different wavelength ranges using last generation evolutionary population synthesis codes. The FIR luminosity produced by the heated dust in star forming regions is commonly used to characterize a starburst. The X-ray luminosity has been found to show a narrow correlation with it, and therefore it has been proposed as an additional tracer of potential interest for high z galaxies, whose FIR emission is redshifted to the sub-mm range. In this communication we analyze the evolution of the X-ray to FIR luminosities ratio as predicted by the CMHK population synthesis models, both for constant stellar formation and instantaneous bursts. The results are compared to some sample data taken from the literature. The conclusion drawn from the comparison is that the empirical calibration of the soft X-ray luminosity seems a valid SFR tracer only for starbursts around a rather short period of time.

1. The L_X/L_{FIR} ratio

We have computed the X-ray and far infrared (FIR) luminosities expected in a massive, young starburst using the CMHK (Cerviño, Mas-Hesse & Kunth) synthesis population models (Cerviño & Mas-Hesse 1994; Cerviño, Mas-Hesse, & Kunth 2002). A Salpeter Initial Mass Function ($\phi(m) \sim m^{-2.35}$) has been assumed, with masses within the range 2–120 M_\odot , 2 different star formation regimes – instantaneous burst (IB) or constant star formation rate (CSFR) – and solar metallicities. We have analyzed the first 30 Myrs after the onset of a massive starburst episode.

The X-ray luminosity is calculated in the range 0.4–2.4 keV. The models compute only the emission by the diffuse gas heated by the mechanical energy released by stellar winds and supernova remnants. The X-ray emission is modeled by Raymond-Smith thermal plasmas with a range of temperatures typical of starburst galaxies (between 0.5 and 1.0 keV). The fraction of mechanical energy ϵ_{eff} effectively heating the gas up to X-rays temperatures is left as a free parameter. The contribution by X-ray binaries and stellar atmospheres has not been considered, since it should be negligible (Cerviño et al. 2002).

A thermal equilibrium of dust has been assumed, which implies all energy absorbed by dust being reemitted in the far infrared range. The models assume that a fraction $(1 - f)$ of Lyman continuum photons are directly absorbed by the dust. The absorption of UV–optical continuum photons is parameterized through $E(B - V)$. The values considered were $f = 0.3$ and $E(B - V) = 1$.

Figure 1 shows the evolution of the soft X-ray luminosity and the L_X/L_{FIR} ratio, as predicted by the models assuming different star formation regimes and efficiencies. We want to stress that this ratio is strongly dependent on the evolutionary state of the starburst, spanning around 2 orders of magnitude within few million years.

The data samples from Ranalli, Comastri, & Setti (2003) and Tüllmann et al. (2006) (hereinafter, *Ran* and *Tul* respectively) were chosen in order to compare with the predictions from the models. As shown in the bottom panels of Figure 1, the observational ratios can be well reproduced by the synthesis models considering efficiency values in the range $\epsilon_{\text{eff}} = 0.01\text{--}0.1$, typical of starburst galaxies (Cerviño et al. 2002). Moreover, our results show that the dispersion observed in the samples ratios can be explained as being mostly an evolutionary effect.

Therefore we conclude that the empirical calibration of the soft X-ray luminosity as an SFR (star formation rate) tracer has to be taken with care, since it would be valid only for starbursts around a relatively short period of time.

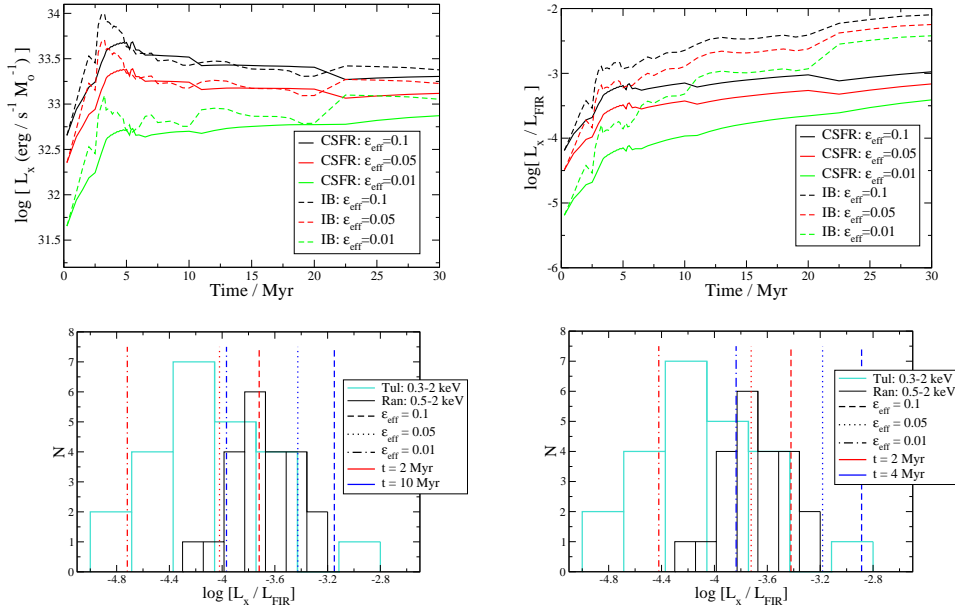


Figure 1. Evolution of L_X (top left) and L_X to L_{FIR} ratio (top right) predicted by the synthesis models. Histograms of the L_X to L_{FIR} ratio for the samples *Ran* and *Tul* considered, together with model predictions: CSFR (bottom left) and IB (bottom right) cases.

References

- Cerviño, M., & Mas-Hesse, J. M. 1994, *A&A*, 284, 749
 Cerviño, M., Mas-Hesse, J. M., & Kunth, D. 2002, *A&A*, 392, 19
 Ranalli, P., Comastri, A., & Setti, G. 2003, *A&A*, 399, 39
 Tüllmann, R., Breitschwerdt, D., Rossa, J., et al. 2006, *A&A*, 457, 779